

REFINEMENT OF THE CRYSTAL STRUCTURE
OF JOHANNSENITE

R. L. FREED AND DONALD R. PEACOR

*Department of Geology and Mineralogy, The University of Michigan,
Ann Arbor, Michigan.*

ABSTRACT

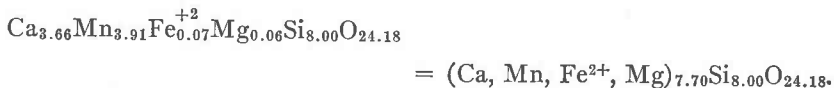
The crystal structure of johannsenite, $4(\text{CaMnSi}_2\text{O}_6)$, with $a=9.978 \text{ \AA} \pm 0.009$, $b=9.156 \text{ \AA} \pm 0.009$, $c=5.293 \text{ \AA} \pm 0.005$, $\beta=105^\circ 29' \pm 02'$, and with space group $C2/c$ was refined by least-squares methods using the Warren and Bragg (1928) diopside structure as a trial model. The refined structure is similar to the Warren and Bragg model. However, the presence of two ordered large cations combined with a zweierketten arrangement of tetrahedra produces distortion in the tetrahedral chain, making it less stable than other metasilicates. The internal strain is compensated by slight offsets of the tetrahedral chains within the close-packed planes, and by twinning with a^* as the twin axis.

INTRODUCTION

W. T. Schaller (1938) gave the first description of johannsenite and stated that X-ray powder photographs show that johannsenite, diopside, and hedenbergite are isostructural. Schiavinato (1953) confirmed these results and gave X-ray powder data (small number of spacings) for diopside and johannsenite. C. Osborne Hutton (1956) gave more complete powder X-ray data for a ferroan johannsenite from Broken Hill, Australia. In this paper the results of a more detailed analysis are given.

COMPOSITION, UNIT CELL, AND SPACE GROUP

The crystal used in this study was selected from material kindly supplied by Waldemar T. Schaller. It is from the Schio-Roebling specimen, Roebling Collection, U. S. Nat. Mus. Cat. No. R3118, and it was collected at the Schio-Vincenti mine, Venetia, northern Italy. A chemical analysis of this specimen is given by Schaller (1938, Table 2, no. 1). The X-ray work for the present study was performed with this analyzed type material. The unit cell contents correspond to the following formula:



These cell contents are normalized to 8.00 Si atoms per cell because a precise specific gravity was not available for this material. Schaller (1938, Table 4, no. 1) gave the ratios of the recalculated analysis for this sample as follows:

Contribution No. 280, Mineralogical Laboratory, Department of Geology and Mineralogy, The University of Michigan, Ann Arbor, Michigan.



with the high SiO_2 value ascribed to admixed quartz, and the low CaO value to admixed rhodonite. The specimen used in this study has the lowest MgO plus FeO content of those analyses listed by Schaller (1938), Schiavinato (1953), Allen and Fahey (1953), Hutton (1956), and Simons and Munson (1963).

Final cell parameters (Table 1) were obtained by least-squares refinement (Burnham, 1962a) of data from *b*- and *c*-axis zero-level Weissenberg photographs. The cell parameters for johannsenite (this paper) and diopside (Warren and Bragg, 1928) are compared in Table 1.

The systematic absences of hkl if $h+k \neq 2n$, and $h0l$ absent if $l \neq 2n$ as

TABLE 1. CRYSTALLOGRAPHIC DATA FOR JOHANNSENITE AND DIOPSIDE

	Diopside (Warren and Bragg, 1928)	Johannsenite (This paper)
<i>a</i>	9.71 Å	9.978 Å ± 0.009
<i>b</i>	8.89	9.156 ± 0.009
<i>c</i>	5.24	5.293 ± 0.005
β	105°50'	105°29' ± 02'
<i>Z</i>	4	4
Space Group	<i>C2/c</i>	<i>C2/c</i>

shown by *b*-axis and *c*-axis Weissenberg photographs are characteristic of space groups *C2/c* or *Cc*. Several photographs were overexposed, but no reflections were observed which violated the above rules. The centrosymmetric space group was chosen due to the suggested isostructural relation of diopside and johannsenite.

INTENSITY DATA

The specimen used for intensity measurements was a prismatic cleavage fragment 0.173 mm long parallel to *c*, and 0.074 × 0.033 mm in cross section. The crystal was mounted with the *c*-axis as the rotation axis. Intensities were gathered using a proportional detector and an equi-inclination counter-diffractometer. All observations were recorded both graphically and by a direct count method. Mechanical considerations reduced the number of nonequivalent observable peaks from 481 to 398.

Intensity values, *I*, were corrected for background from determinations of the average value of measurements on both sides of the peak and the total intensity value measured by scanning the peak. The background, absorption, and Lorentz-polarization corrections were computed

in modified versions of IBM 7090 Fortran II programs written by C. T. Prewitt (1964) and C. W. Burnham (1962b).

Several weighting schemes for use in least-squares refinement were tested. The first was based on the standard deviations calculated from the original intensities:

$$\begin{aligned}\sigma(I) &= 0.675 [I(\text{total}) + I(\text{background})]^{\frac{1}{2}} \\ \sigma(F^2) &= K\sigma(I),\end{aligned}$$

where K is a constant determined by the product of a scale factor, the transmission factor, and Lorentz-polarization factors. This weighting scheme results in a stronger weighting of the stronger substructure reflections relative to that of the weaker superstructure reflections. However, the effects of primary extinction would result in erroneous weights for the larger intensity values. The data used in this study did not appear to be greatly affected by this problem.

The second scheme used (Cruickshank, *et al* 1960) may be written:

$$\sigma^2 = 2a + |F_o| + b(F_o)^2$$

where $a = 2|F_{\min}|$, and $b = 2/|F_{\max}|$. Intensity values in the "medium" range will be, in effect, weighted stronger relative to strong or weak reflections.

This laboratory has found that a simple one-to-one combination of both schemes results in better standard deviations of the atom parameters than those obtained by using the two schemes separately.

It was extremely difficult to find a cleavage fragment acceptable for X-ray work from any of the material at our disposal. All crystals were affected to some degree by lineage structure and twinning. The lineage structure was especially prominent in those reciprocal-space directions near the b^* and c^* directions. Therefore, when a crystal which gave an acceptable peak profile was found, it was used for the collection of data even though it was twinned. The fact that the twinning could not be detected optically indicated that the twin "domains" were small and an acceptable absorption correction could be applied to the crystal as a whole. X-ray photographs showed that one twin component was very small in comparison with the twin-related component.

The twinning occurs with a^* as the twin-axis. Thus, with the crystal mounted on the c -axis, reflections from both twin members will appear on odd-levels as single reflections. Even-levels have reflections from individual twin-related elements superimposed on each other. The problem becomes the task of calculating the twin volume relation in order to correct the even-level intensities. This was attempted by direct counting of

equivalent odd-level reflections, but due to the large difference in relative sizes of the twins, only fourteen peaks were observable. Calculations based on these observations gave an average twin volume factor equal to 0.0238. Individual volume factors ranged from 0.0134 to 0.0398. The average value obtained from this method was considered too unreliable to be used for data correction. Therefore, a least-squares correction was employed as described below.

An observed even-level intensity, I_0 , would be the sum of the component from the twinned member, I_B , and that from the twin-related member, I_A . The twinned and twin-related members will have the same k and l values, but in general $h_A \neq h_B$. For any two twin related observed even-level intensities:

$$I_A(H) + I_B(h) = I_0(H) \quad (1)$$

$$I_A(h) + I_B(H) = I_0(h) \quad (2)$$

where (H) and (h) are related by the twin-axis a^* .

Each intensity I_A is related to its twin-related intensity I_B by a proportionality constant, K , such that $I_B(H) = KI_A(H)$ and $I_B(h) = KI_A(h)$. The constant, K , is the twin volume factor. By use of these relations, equations (1) and (2) can be combined to give:

$$I_A(H) = [I_0(H) - KI_0(h)]/[1 - K^2] \quad (3)$$

which may be rewritten

$$I_A(H) = K_1 I_0(H) - K_2 I_0(h) \quad (3a),$$

where $K = K_2/K_1$.

Least-squares techniques were applied to equation (3a) resulting in a pair of equations which relate $I_A(H)$ (which is the desired corrected even-level intensity value), K_1 and K_2 (and thus K), and the original observed intensities. The procedure was to start with an approximate value for $I_A(H)$ and the original observed intensities, and use the least-squares equations to calculate K_1 and K_2 . Equation (3a) was then used to find a new $I_A(H)$ which was used in the structure refinement. The structure was refined, a list of calculated structure factors was generated, and these calculated values were then used as new approximate $I_A(H)$ values. This procedure was employed five times during the structure refinement. A final twin volume ratio $K = 0.0674$ was calculated. This value was used in equation (3) to calculate a final set of $I_A(H)$ values.

REFINEMENT

A modified version of an IBM 7090 Fortran II program written by C. T. Prewitt (1962) was used to refine the atom parameters by a least-

squares method using the full matrix. All atoms were assumed half-ionized and a correction was made for the average real and imaginary components of anomalous dispersion. An overall isotropic temperature factor of 1.0 was initially employed. All $F_0=0$ were not used in the refinement, but they were used to calculate the discrepancy factor, R .

Initial atom parameters were taken from Warren and Bragg (1928). Ideal diopside contains two crystallographically distinct cations occurring in a one-to-one ratio. Johannsenite also contains two cations which are present in approximately equal amounts. Therefore, it is reasonable to assign crystallographically distinct sites for both types of cations of johannsenite. The diopside structure has these two cations occupying equipoints of rank 4. If the Ca atoms of johannsenite are assumed to occupy Ca sites of diopside, then the Mn atoms will occupy the Mg atom positions. Both Fe^{+2} and Mg are relatively small cations and it is reasonable to assume that they will go into the smaller cation site. The manganese form factor curve was corrected for the iron and magnesium known to be present. This assumption was checked and verified periodically by refining "population densities."

Refinement began with only odd-level data, and the first weighting scheme described above. A single scale factor and the atom parameters were allowed to vary, and the value of the discrepancy factor $R(\text{weighted})$ decreased rapidly to 9.5 percent.

The even-level data were included and refinement proceeded as above, except that two scale factors were employed: one each for odd-level and even-level data. The $R(\text{weighted})$ value initial increased to 11.0 percent. From this point the corrections for twinning discussed above were employed. Two questionable reflections showing primary extinction were eliminated, and one was removed which appeared to be erroneously recorded.

The isotropic temperature factors for each atom were allowed to vary with fixed atom coordinates. The isotropic temperature factor value for O(3) immediately went negative. Several attempts at refinement still yielded a negative O(3) isotropic temperature factor.

The weighting scheme given by Cruickshank, *et al* (1960) was then employed. The positional parameters changed slightly, but the standard deviations improved by a factor of nearly two. All of the isotropic temperature factors became positive. These parameters (positional and temperature) were used to calculate structure factors which in turn were used to make a final twin volume correction.

The final weighting scheme (see Intensity Data) produced very little change in the positional parameters and essentially no change in their standard deviations. However, the isotropic temperature factors im-

proved, and their standard deviations decreased to approximately three-fourths the previous value. An attempt was made to refine anisotropic temperature factors, but this was unsuccessful. The final parameters and their standard deviations are listed in Table 2. The value of the final discrepancy factor, R , was 6.6 percent. Table 5¹ lists the observed and final calculated structure factors of johannsenite.

RESULTS

Johannsenite and diopside are isostructural. Figure 1 compares both minerals drawn in projection along the b -axis. Only a half cell is shown for each structure. Atom positions are slightly different, but not enough to affect the basic structural similarity. Selected bond lengths and angles are

TABLE 2. ATOM COORDINATES AND ISOTROPIC TEMPERATURE FACTORS FOR JOHANNSENITE. STANDARD DEVIATIONS ARE GIVEN IN PARENTHESES

Atom	x	y	z	B
Ca	0	0.6981 (0.0002)	3/4	0.58 (0.03)
Mn	0	.0947 (0.0002)	3/4	.48 (0.03)
Si	0.2129 (0.0002)	.4083 (0.0002)	0.7637 (0.0004)	.26 (0.03)
O (1)	.3797 (0.0006)	.4070 (0.0005)	.8459 (0.0011)	.39 (0.08)
O (2)	.1368 (0.0005)	.2569 (0.0006)	.6705 (0.0010)	.47 (0.09)
O (3)	.1518 (0.0007)	.4794 (0.0006)	.0043 (0.0012)	0.40 (0.10)

given in Table 3, and were computed with an IBM 7090 Fortran II program written by W. R. Busing, K. O. Martin, and H. A. Levy (1964).

The main features of pyroxene structures have been known for some time and a survey of these are given by Prewitt and Peacor (1964). Therefore, only a brief discussion will be given here.

Johannsenite has a zweierketten tetrahedral repeat unit which classifies it as a so-called true pyroxene. The tetrahedrally-coordinated sites alternate with octahedrally-coordinated sites between sheets of close-packed oxygen layers. These oxygen layers are parallel to the (100) plane. The octahedra share edges to form bands parallel to the silicate chains. However, there is a rift in the octahedral layer which is enclosed by two parallel silicate chains with chain-vertices pointing away from each other. The tetrahedrally-coordinated layer has parallel continuous chains

¹ Table 5, listing observed and final calculated structure factors of johannsenite, has been deposited as Document No. 9356 with the American Documentation Institute, Auxiliary Publications Project, Photoduplication Service, Library of Congress, Washington 25, D. C. Copies may be secured by citing the document number, and remitting in advance. \$1.25 for photoprints or \$1.25 for 35 mm microfilm.

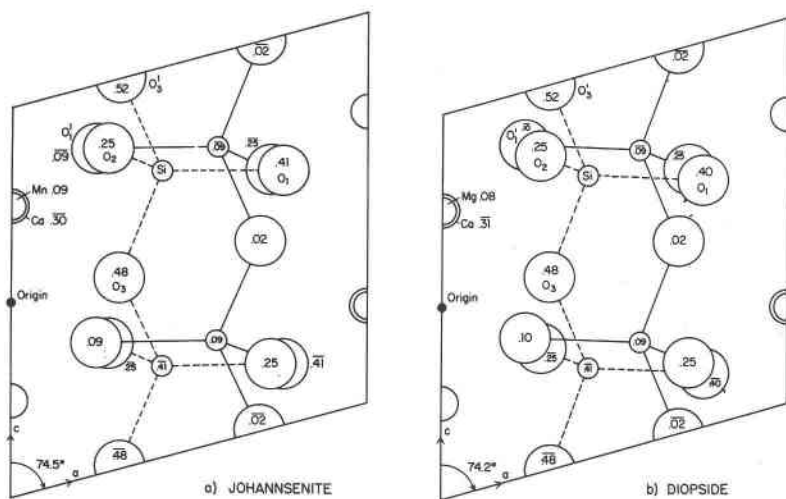


FIG. 1. Crystal structures of johannsenite and diopside projected along the *b*-axis. Only a half-cell of each mineral is shown. Numbers represent heights of atoms above and below the (020) plane.

TABLE 3. SELECTED INTERATOMIC DISTANCES AND ANGLES OF JOHANNSENITE. STANDARD DEVIATIONS ARE IN PARENTHESIS.¹ ALL DISTANCES ARE IN ÅNGSTRÖMS; ANGLES ARE IN DEGREES

Ca-O		Si-O		Mn-O	
2	O(1) 2.384 (.006)	O(1)	1.604 (0.006)	2	O(1) 2.155 (0.006)
2	O(2) 2.316 (.006)	O(2)	1.594 (0.006)	2	O(1)' 2.231 (0.006)
2	O(3) 2.651 (.007)	O(3)'	1.693 (0.007)	2	O(2) 2.134 (0.006)
2	O(3)' 2.771 (.006)	O(3)	1.683 (0.007)		
avg.	2.53	avg.	1.64	avg.	2.17
O—O in tetrahedra			Angles		
O(1)	—O(2)	2.725	(0.008)	O(1) —Si —O(2)	116.84 (0.27)
O(1)	—O(3)'	2.707	(0.009)	O(1) —Si —O(3)'	110.32 (0.31)
O(1)	—O(3)	2.708	(0.008)	O(1) —Si —O(3)''	110.92 (0.31)
O(2)	—O(3)'	2.588	(0.008)	O(2) —Si —O(3)'	103.80 (0.30)
O(1)	—O(3)	2.675	(0.008)	O(2) —Si —O(3)	109.37 (0.29)
O(3)'	O(3)	2.673	(0.003)	O(3)' —Si —O(3)	104.71 (0.24)
				O(3) —O(3)' —O(3)''	163.78 (0.47)
				Si —O(3)' —Si	136.37 (0.41)
Si—Si					
Si—Si'	3.134 (0.003)				

¹ The standard deviations do not directly include errors involved in the calculation of the twin volume factor, or systematic errors due to the twinning.

with chain-vertices pointing alternately in opposite directions. Figure 2 shows a projection of the structure of johannsenite looking directly down on the close-packed layers. Those chains with vertices "up" have bases which parallel the above mentioned rift in the octahedrally-coordinated layer.

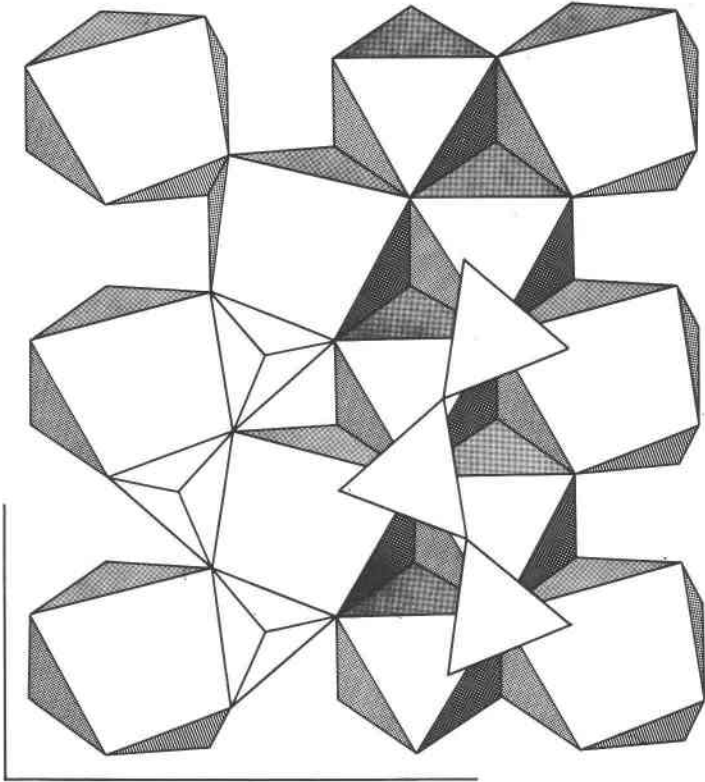


FIG. 2. The johannsenite structure projected onto a plane parallel to the close-packed oxygen layers. Unit translations are shown in the lower left of the figure. A single octahedral layer and a portion of the adjacent tetrahedral layer are shown. The shaded areas represent planes which are sloping away from the viewer.

There are two kinds of octahedrally-coordinated sites. The first, M(2), is occupied by Ca atoms and has approximate 8-fold coordination which forms a nonregular coordination polyhedron. The second site, M(1), is occupied by Mn atoms and has 6-fold coordination which forms a regular octahedron. Figure 2 illustrates the coordination features for M(1) and M(2). The nonregular polyhedra on the left and right margins of the figure are polyhedra associated with the M(2) sites. The regular

octahedra associated with the M(1) sites follow the chain of tetrahedra on the right-hand side of the diagram.

Table 4 is a modified extension of a table given by Morimoto, Appleman and Evans (1960, Table 6) relating the distribution of metal atoms between the M(1) and M(2) sites, the coordination numbers of the metal atoms, and the average metal—oxygen atomic distances. Clinoenstatite, pigeonite, and diopside have Ca, Fe⁺², and Mg atoms in an almost completely ordered state. The data of Table 4 illustrates that Ca and Mn atoms of johannsenite are also ordered, and helps to show that the refined structure of johannsenite verifies the conclusions reached earlier concern-

TABLE 4. RELATIONS OF THE METAL ATOMS IN CLINOENSTATITE, PIGEONITE, DIOPSIDE AND JOHANNSENITE

Designation		Atoms	Coordination number	Avg. M—O distances
Clinoenstatite (Morimoto <i>et al.</i> , 1960)	M(2)	Mg	6	2.15 Å
	M(1)	Mg	6	2.07
Pigeonite (Morimoto <i>et al.</i> , 1960)	M(2)	Ca _{0.20} Fe _{0.80}	7	2.36
	M(1)	Mg _{0.68} Fe _{0.32}	6	2.11
Diopside (Warren and Bragg, 1928)	M(2)	Ca	8	2.50
	M(1)	Mg	6	2.12
Johannsenite (This paper)	M(2)	Ca	8	2.53
	M(1)	Mn	6	2.17

ing ordering in johannsenite. It seems reasonable to propose that complete solid solution exists between johannsenite and diopside. The coordination of the M(1) and M(2) sites remain the same, and the only change is a constant variation in the amount of Mg and Mn atoms in the M(1) site.

Valency sums may be calculated for each oxygen atom by assuming a bond strength of 1/4 for each Ca—O bond, 1/3 for each Mn—O bond, and 1 for each Si—O bond. Oxygen O(1) is coordinated to 1 Si, 1 Ca, and 2 Mn atoms for a total bond strength of 1-11/12. Oxygen O(2) is coordinated to 1 Si, 1 Mn, and 1 Ca atoms for a total bond strength of 1-7/12. Oxygen O(3) is coordinated to 2 Si, and 2 Ca atoms for a total bond strength of 2-1/2. These deviations from the ideal situation are compensated, in general, by lengthening of Ca—O(3) and Si—O(3) bonds, "normal" Ca—O(1) and Si—O(1) bond lengths, and a shortening of Ca—O(2) and Si—O(2) bonds. Mn—O bonds are generally uniform.

DISCUSSION

The configuration of the tetrahedral chains in pyroxenes and related structures has been discussed by Liebau (1962) and Prewitt and Peacor (1964). It was noted that the chain configuration is apparently a function of the average size of the octahedrally-coordinated cations. This occurs because those oxygen atoms which are positioned at the chain-vertices are also positioned at the junctions of the vertices of an edge-sharing band of octahedra. Thus, the geometry of the tetrahedron arrangement is affected by the relative size of the octahedra. This relation is quite similar to a corresponding one in the phyllosilicates.

The zweierketten repeat unit is controlled by the relative size of the M(1) octahedron. As the average radius of the M(1) cation increases, the stability of the pyroxene (zweierketten) structure should decrease relative to that of a pyroxenoid with a repeat unit of 3, 5, or 7 tetrahedra in the chain.

The major phases in the $\text{CaSiO}_3\text{-MnSiO}_3$ system are wollastonite (CaSiO_3 , dreierketten), rhodonite (MnSiO_3 , funferketten), and bustamite ($\text{CaMnSi}_2\text{O}_6$, dreierketten). Johannsenite apparently has a very limited solid solution range in this system and inverts to bustamite at about 830°C (Schaller, 1938). The relative stability of diopside (Mg in the M(1) site) is shown in that it does not change up to the melting point. Thus, it seems reasonable to expect some deviations from the normal pyroxene (diopside) structural features in compensation for the large Mn cation in the M(1) site.

The large Si-O(3) and Si-O(3)', distances are immediately evident upon examination of Table 3. These values are thought to be due to a combination of two related factors: 1) the presence of Mn in the M(1) site forces the tetrahedral chain to be distorted, as shown by the O(3)-O(3)'-O(3)'' angle of 163.8° , and 2) the relatively large c translation (5.293 \AA) requires larger than normal Si-O distances along the chain axis.

The tetrahedral angles are given in Table 3. The effect of Mn in the structure may be considered to produce an expansion of the tetrahedra in the chain direction, with a corresponding decrease of the tetrahedra size in the other directions. The smaller Si-O(1) and Si-O(2) distances combine with the larger distances to give an average Si-O value of 1.64 \AA , which is larger than the value of 1.623 \AA predicted by Smith and Bailey (1963) for metasilicates. This large average value for johannsenite is reasonable in light of the above discussion, and also after considering that the two smaller Si-O distances tend to compensate for the larger distances even though the O(1) and O(2) positions are strongly affected by the presence of two large cations.

The apparently limited solid solution range for johannsenite in the

$\text{CaSiO}_3\text{-MnSiO}_3$ system can be explained in general terms by the requirement of cation ordering. This would also qualitatively explain why the published analyses of johannsenite have an approximate one-to-one ratio of Ca atoms to the sum of Mn, Mg, and Fe^{+2} atoms.

Bustamite (Peacor and Buerger, 1962) also has cation ordering, but the number of non-equivalent cation positions increases from two to four. Johannsenite has a double band of octahedra paralleling the tetrahedral chain (see Fig. 2), but bustamite has a triple band. Another difference is that the tetrahedral chain in johannsenite should make an angle of approximately 30° to the chain in bustamite if it is assumed that the b -axes are parallel and the close-packed layers have a similar orientation. Thus, the johannsenite-bustamite inversion mentioned above involves a major change in the geometry of the tetrahedral chain, and also in the arrangement of cations in the octahedral layer.

It was shown above that the M(1) site controls the chain configuration of johannsenite. It seems reasonable then to expect the inversion to bustamite to affect this M(1) site to a marked degree. The effect of Mn in the M(1) site has already been discussed. If an even larger cation were to occupy that site, a further distortion of the chain configuration could be expected, even to the extent of destroying the zweierketten repeat unit.

The inversion of johannsenite to bustamite may involve just such a situation. Rising temperature may lead to disorder. In that case, some Ca atoms would occupy the M(1) site. This would produce a distortion of both the tetrahedral chain configuration and the octahedral sheet. As mentioned earlier, a pyroxenoid structure should have greater stability if a large cation were to occupy the M(1) site. Thus, the disorder of cations in johannsenite might lead to a more stable structure having a dreierketten repeat unit and four nonequivalent cation sites.

Two other features may indicate that the johannsenite structure is less stable than other pyroxene and related structures. Lineage structure was the first limiting factor in finding a crystal suitable for X-ray work, and it was noted that the strongest effects occurred in those reciprocal-space directions near the b^* and c^* directions. This might be due to slight offsets along the tetrahedral chain axis within the close-packing plane. These offsets would help to compensate for any internal strain.

The second factor in finding a crystal was the twinning. The twin-axis a^* is normal to the close-packed oxygen layers. The twinning in johannsenite might be simply a variation in the stacking sequence of the close-packed oxygen layers. The plane of twinning would most likely be the plane containing the octahedrally-coordinated sites. The configuration of the cations would remain approximately the same, but the oxygens would assume the second alternative for stacking close-packed layers.

ACKNOWLEDGEMENTS

This work was sponsored by a grant from the National Science Foundation. Computations were performed in part on the IBM 7090 computer at The University of Michigan Computing Center. Dr. Waldemar T. Schaller was extremely helpful by kindly supplying crystals from all of the type analyzed material described in his 1938 paper.

REFERENCES

- ALLEN, V. T. AND J. J. FAHEY (1953) Rhodonite, johannsenite and ferroan johannsenite at Vanadium, New Mexico. *Amer. Mineral.* **38**, 883-890.
- BURNHAM, CHARLES W. (1962a) LCLSQ, crystallographic lattice-constant least-squares refinement program. *Carnegie Inst. Wash. Year Book* **61**, 132-135.
- (1962b) Absorption corrections for prismatic crystals and evaluation of end affect. (Abstr.) Meet. *Amer. Crystallogr. Soc.* 1962 p. 19.
- BUSING, W. R., K. O. MARTIN AND H. A. LEVY (1964) OR FFE, A Fortran Crystallographic function and error program. *Oak Ridge Nat. Lab.* [Oak Ridge, Tenn.] *Rep.* **TM-306**.
- CRUICKSHANK, D. W. J., DIANA E. PILLING, A. BUJOSA, F. M. LOVELL AND MARY R. TRUTER (1960) Crystallographic calculations on the Ferranti Pegasus and Mark I computers. In *Computing Methods and the Phase Problem in X-Ray Crystal Analysis*. Pergamon Press, N. Y., p. 32-78.
- HUTTON, C. OSBORNE (1956) Manganpyrosmalite, bustamite, and ferroan johannsenite from Broken Hill, New South Wales, Australia. *Amer. Mineral.* **41**, 581-591.
- LIEBAU, F. (1962) Die Systematik der Silikate. *Naturwissenschaften* **49**, 481-491.
- MORIMOTO, NOBUO, DANIEL E. APPELMAN AND HOWARD T. EVANS, JR. (1960) The crystal structures of clinoenstatite and pigeonite. *Z. Kristallogr.* **114**, 120-147.
- PEACOR, DONALD R. AND M. J. BUERGER (1962) Determination and refinement of the crystal structure of bustamite, $\text{CaMnSi}_2\text{O}_8$. *Z. Kristallogr.* **117**, 331-343.
- PREWITT, C. T. (1962) *SFLSQ2*, an IBM 7090 program for least-squares refinement. Ph.D. Thesis. Mass. Inst. Tech.
- (1964) *DFSET4*, a program for computing equi-inclination-diffractometer settings. Central Research Department, Experimental Station, E. I. Du Pont, De Nemours and Co.
- AND DONALD R. PEACOR (1964) Crystal chemistry of the pyroxenes and pyroxenoids. *Amer. Mineral.* **49**, 1527-1542.
- SCHALLER, WALDEMAR T. (1938) Johannsenite, a new manganese pyroxene. *Amer. Mineral.* **23**, 575-582.
- SCHIAVINATO, G. (1953) Sulla johannsenite dei giacimenti a silicati manegnesferi del Monte Civillina presso Recoaro (Vincenza). *Rend. Soc. Mineral. Ital.* **9**, 210-218.
- SIMONS, FRANK S. AND ELAINE MUNSON (1963) Johannsenite from the Aravaipa mining district, Arizona. *Amer. Mineral.* **48**, 1154-1158.
- SMITH, J. V. AND S. W. BAILEY (1963) Second review of Al-O and Si-O tetrahedral distances. *Acta Crystallogr.* **16**, 801-811.
- WARREN, B. AND W. LAWRENCE BRAGG (1928) The structure of diopside. *Z. Kristallogr.* **69**, 168-193.

Manuscript received, June 8, 1966; accepted for publication, September 8, 1966.